Available online at www.sciencedirect.com
ScienceDirect
Journal of Power Sources 179 (2008) 799–807
JOURNAL OF POWER SOURCES
www.elsevier.com/locate/jpowsour

New approach to prevent premature capacity loss of lead-acid battery in cycle use

Ken Sawai *, Yuichi Tsuboi, Yuichi Okada, Masaaki Shiomi, Shigeharu Osumi

Technical Development Division, Industry Business Unit, GS Yuasa Power Supply Ltd., Nishinosho, Kisshoin, Minami-ku, Kyoto 601-8520, Japan

Received 3 December 2007; accepted 20 December 2007
Available online 9 January 2008

Abstract

Pb–Ca foil laminated on rolled sheet for positive grid of lead-acid battery is proposed to prevent premature capacity loss (PCL) during charge–discharge cycling. Batteries with Pb–Ca foil laminated on positive grid had longer life during charge–discharge cycle than conventional battery, which failed early by PCL. PCL is a phenomenon due to the increase of the interfacial resistance between the positive grid and the positive active mass (PAM) during discharging by $PbSO_4$ formation in the corrosion layer. Positive plates suffered from PCL when the compression between the grid and the PAM was poor, H_2SO_4 concentration at the interface was high or the corrosion layer mainly consisted of β-PbO_2. Adhesion between the PAM and Pb–5%Sb alloy or Pb–1%Ca alloy was firmer than that between the PAM and Pb–0.06%Ca–1.5%Sn. Corrosion layer formed at the interface between grid material and the PAM during cycle included more α-PbO_2 on Pb–5%Sb and on Pb–1%Ca than on Pb–0.06%Ca–1.5%Sn. It was found out that excellent cycle life performance with Pb–1%Ca foil against PCL is due to firm adhesion between the PAM and grid material, and that α-PbO_2 is formed at the interface as a result of firm adhesion of the PAM and Pb–1%Ca grid.

Keywords: Lead-acid battery; Premature capacity loss (PCL); Positive plate; Grid; Laminate

1. Introduction

It is well known that some valve-regulated lead-acid (VRLA) batteries with antimony-free positive grid lose discharge capacity earlier than expected under certain conditions, even in a floating application [1–3]. This phenomenon is called "premature capacity loss (PCL)". PCL is caused by the capacity loss of the positive plates, typically during deep discharge and full charge cycle [3]. Discharge capacity of the battery with pure Pb grid plates decreased after a few cycles because the grid surface was passivated with corrosion layer during cycling, although it did not decline with Pb–Sb grid plates and the grid surface was not passivated [4,5]. It means that if the positive grid includes Sb in its composition, PCL is prevented. On the other hand, Sb is oxidized and the ion is dissolved into the electrolyte [6] and precipitates on the negative electrode as Sb metal during cycling. It lowers the hydrogen overpotential of the negative electrode and causes more water loss and dry out of the cell [7]. Therefore, a number of studies have been carried out to prevent PCL with antimony-free positive grid so far.

Large current charging was found to delay PCL [5,8,9]. A barrier layer formed on a Pb–Ca–Sn grid during discharging was found to be $PbSO_4$ when PCL occurred [8,10,11]. These papers mentioned above dealt with the interface between the grid and the positive active mass (PAM).

On the other hand, there were papers dealing with PAM characteristics, especially changes in the connection or the size of the PAM particles, which was affected by the charging conditions [12–15]. These papers described how PCL phenomenon was caused by increase of positive plate resistance. However, PCL mechanism is different in each paper.

In the former report [2], PCL was found to be a phenomenon due to the increase of the interfacial resistance between the grid and the PAM by the direct measurements of resistance across the interface and in the PAM.

* Corresponding author. Tel.: +81 75 312 2123; fax: +81 75 316 3798.
E-mail address: ken.sawai@jp.gs-yuasa.com (K. Sawai).

0378-7753/$ – see front matter © 2007 Elsevier B.V. All rights reserved.
doi:10.1016/j.jpowsour.2007.12.106

Effects of Sb addition to prevent PCL are explained by change of corrosion layer in physical and chemical characteristics.

Oxide layer formed on Pb–Sb alloy is hard to crack, while that formed on Pb metal is dense and crack and come off easily [16]. Oxide layer formed on Pb–Sb is thicker and includes more water than that formed on Pb [17]. The texture of oxide layer surface is finer on Pb–Sb than on Pb [18].

Another effect of oxide layer including Sb is to improve the electrical conductivity [19,20]. It is supposed that conductivity of gel of Pb–O–Pb chain structure [21] increases more, or PbO_x is formed more in the interfacial layer by oxidation of t-PbO [22] on Pb–Sb rather than on Pb.

Other papers reported that oxide layer including Sb consists of α-PbO_2 [23], and α-PbO_2 becomes more stable with Sb doped [3]. In acidic solution, β-PbO_2 is more stable than α-PbO_2, but is rapidly reduced to $PbSO_4$ [24]. Therefore, it is supposed that α-PbO_2 becomes stable with Sb and the α-PbO_2 layer keeps the conductive path at the PAM/grid interface from reduction to $PbSO_4$.

In this report, Pb–Ca alloy laminated on rolled sheet for the positive expanded grid is proposed to increase adhesion of the PAM to grid and to control PCL phenomenon.

2. Influence of the interface state between the grid and the PAM on endurance against PCL

A functional electrode and cell were designed and tested to examine the effects of the reactivity of the corrosion layer between the positive grid and the PAM on endurance against PCL.

2.1. Experimental

The PAM paste made from leady oxide powder (raw material of lead-acid battery active material), water and sulfuric acid was filled into a hole (diameter: φ25 mm, thickness: 3 mm) in a resin frame. It was cured under 3BS (tribasic lead sulfate, $3PbO{\cdot}PbSO_4{\cdot}H_2O$) conditions on Pb–0.06%Ca–1.5%Sn sheet. Then, it was formed (oxidized) by electrochemical oxidation to a PAM tablet (density: 3.7 g cm^{-3}) on the Pb–0.06%Ca–1.5%Sn sheet. After formation, this tablet of the PAM was taken off the Pb alloy sheet and its surface was polished to make it smooth. This tablet was put on a Pb–0.06%Ca–1.5%Sn (percentage of alloy composition means mass % in this report) alloy flat current collector, as shown in Fig. 1(a) on which corrosion layer was formed in advance. An absorptive glass mat (AGM) separator, a conventional negative plate and a weight were put on the PAM tablet. 5.26 M H_2SO_4 was poured to be retained in the PAM, AGM and negative active material (NAM) before the weight was put on. Fig. 1(b) shows the construction of the "tablet plate cell".

The resistance of the electrolyte at the interface area between the current collector (Pb alloy) and the PAM can be changed by mass of the weight and by adding a different concentration of electrolyte directly on the corrosion layer.

A light weight means relatively small adhesion between the PAM and the corrosion layer on the current collector. This would cause high mobility and low resistance of H_2SO_4 around the corrosion layer area. Thus, the effect of electrolyte resistance at the interface area on endurance against PCL can be examined with this tablet plate cell.

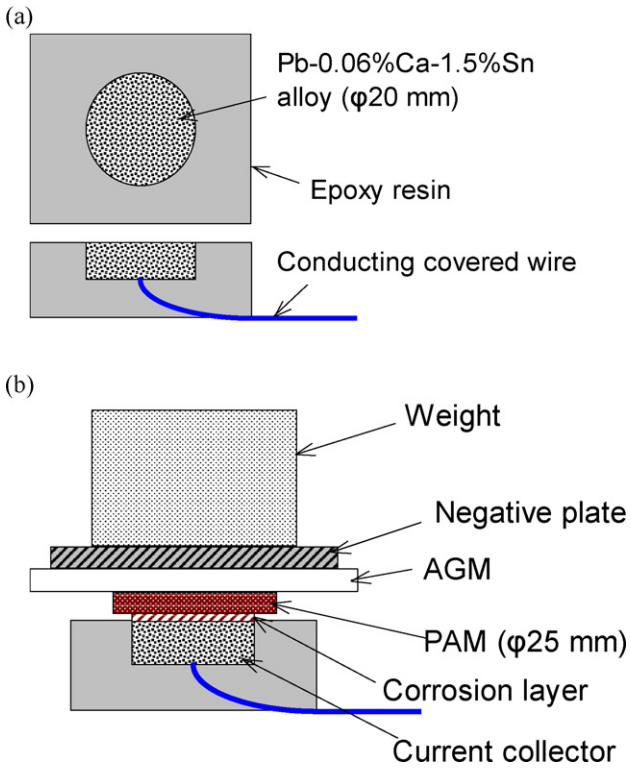

Fig. 1. Schematic diagram of (a) current collector and (b) "tablet plate" cell.

Two different compounds (α-PbO_2 and β-PbO_2) were formed as the corrosion layer by anodic oxidation of the current collector surface before the PAM tablet was put on, in order to examine the effect of the corrosion layer reactivity on PCL phenomenon. In general, it is known that β-PbO_2 is more reactive than α-PbO_2 and shows a higher utilization rate when discharged [24]. In case of conventional positive plates with grid and the PAM, the composition of the corrosion layer cannot be changed without changing other material conditions, such as the PAM composition or physical characteristics. However, with this tablet plate, the composition of the corrosion layer can be changed without changing any other material conditions.

The α-PbO_2 corrosion layer was made by anodic oxidation in 0.1 M NaOH, while the β-PbO_2 corrosion layer was made by anodic oxidation and one discharge–charge cycle in 0.82 M H_2SO_4.

Details of the cell composition are described in Table 1. These cells were discharged at 150 mA (i.e. 27.5 mA g^{-1} of the PAM) at 25–30 °C and discharge voltage was measured.

2.2. Results and discussions

The change of discharge voltage of the cells with various weights is shown in Fig. 2. Voltage of cells with weight of less than 450 g (9.0 kPa compression at interface area) dropped at short time discharge. There were no effects on the cells with the

Table 1
Detail of the tablet paste cells

Cell No.	Corrosion layer	H_2SO_4 concentration (M)		Mass of weight (g)
		In AGM separator, PAM and NAM	Around corrosion layer	
1	β-PbO_2 rich[a]	5.26	5.26	300
2	β-PbO_2 rich	5.26	5.26	450
3	β-PbO_2 rich	5.26	5.26	600
4	β-PbO_2 rich	5.26	5.26	1000
5	β-PbO_2 rich	5.26	5.26	2000
6	β-PbO_2 rich	5.26	7.21	2000
7	α-PbO_2 rich[b]	5.26	7.21	2000

[a] Made by one reduction–oxidation cycle after anodic oxidation (100 mA × 48 h in 0.82 M H_2SO_4).
[b] Made by anodic oxidation: 100 mA × 48 h in 0.1 M NaOH.

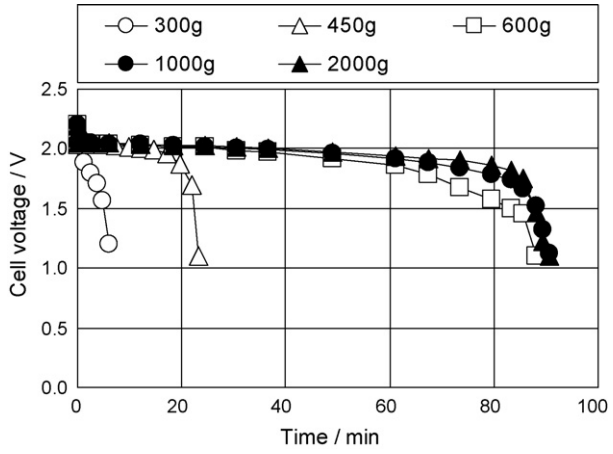

Fig. 2. Discharge characteristics of the "tablet plate cell" at 150 mA, 25–30 °C with a weight of 300 g (◯), 450 g (△), 600 g (□), 1000 g (●), 2000 g (▲) on the plates.

weight of more than 600 g (12 kPa compression). The decline of discharge voltage is not due to just the poor contact between the current collector and the PAM, because the discharge voltages of all the cells at the beginning of discharge are all the same, notwithstanding the weight difference. Therefore, this decline in discharge capacity of the cells with light weight is assumed to be due to PCL phenomenon.

It was found from these results that PCL is largely affected by the adhesion between the PAM and the current collector (β-PbO_2 corrosion layer), and that discharging of the corrosion layer causes the increase of internal resistance during discharge.

The change of discharge voltage of the cells under various interfacial conditions is shown in Fig. 3. The discharge voltage of the positive electrode with 7.21 M H_2SO_4 on the β-PbO_2 corrosion layer (cell No. 6) dropped at shorter time than that with 5.26 M H_2SO_4 (cell No. 5), although the discharge voltages at the beginning of the discharge were not different for the both cells. In this experiment, a 2000 g weight (40 kPa compression) was applied to the cells and they did not fail by poor adhesion. It was found that high concentration H_2SO_4 around the β-PbO_2 corrosion layer accelerate PCL, even if the adhesion is good between the current collector and the PAM. It may be because the electrode potential of the corrosion layer becomes higher and the corrosion layer is preferentially discharged when the H_2SO_4 concentration around the corrosion layer increased.

On the other hand, the positive electrode with 7.21 M H_2SO_4 on the α-PbO_2 corrosion layer (cell No. 7) did not show PCL behavior at all. These experimental results proved that the effect of corrosion layer composition on PCL phenomenon is much larger than that of the local H_2SO_4 concentration. Especially the α-PbO_2 corrosion layer can prevent PCL, even in a high H_2SO_4 concentration around corrosion layer. This may be caused by the reactivity or the electrode potential difference between α-PbO_2 and β-PbO_2.

3. Adhesion between the PAM and grid after the positive plates curing

In the Section 2, PCL was found out to be the phenomenon that the corrosion layer of grid discharges earlier than the PAM to increase the internal resistance of the cell, and it is largely affected by the adhesion between the PAM and the current collector. For the positive plates of the test cells in the Section 2, the adhesion was kept with load of a weight during discharging. However, in lead-acid batteries, it is difficult to keep adhesion by direct compression to the plates. Therefore, it is important to make the adhesion of the PAM to grid tight during the plate manufacturing process.

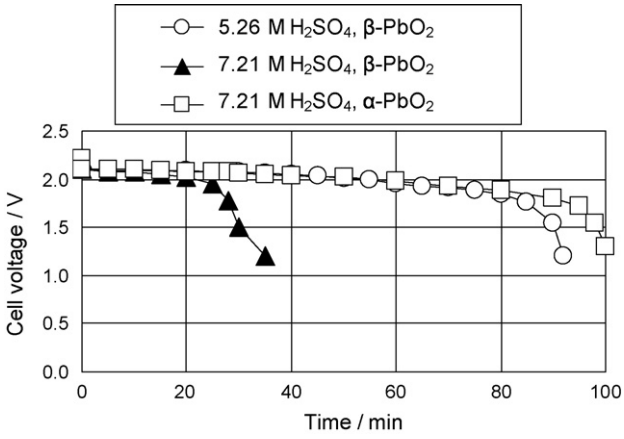

Fig. 3. Discharge characteristics of the "tablet plate cell" at 150 mA, 25–30 °C under various conditions of sulfuric acid concentration at interfacial area and corrosion layer composition on the current collector. The conditions are; 5.26 M H_2SO_4, β-PbO_2 (◯); 7.21 M H_2SO_4, β-PbO_2 (□); 7.21 M H_2SO_4, α-PbO_2 (▲).

Adhesion between the PAM tablet and grid alloy was measured after curing before formation for grid alloy sheets of various composition.

3.1. Experimental

A paste tablet was put on a sheet of grid alloy and cured. The force to take the unformed PAM tablet off the Pb alloy sheet was measured after curing, in place of the adhesion measurement between the PAM tablet and grid alloy. Three types of Pb alloy were tested, Pb–0.06%Ca–1.5%Sn, Pb–1%Ca, and Pb–5%Sb. Test samples were prepared as follows. The schematic diagram is shown in Fig. 4.

(1) 2 mm thick Pb alloy sheet was cut into 20 mm × 20 mm size.
(2) Paste made from leady oxide, sulfuric acid, and water was mixed into paste and filled in 20 mm × 20 mm × 3 mm ABS frame.
(3) The paste tablet was set on the alloy sheet, just after filling.
(4) The paste tablet and sheet sample was cured in 50 °C, 80% relative humidity for 30 min to 72 h with constant compression at 2.45–24.5 kPa by the weight of 100–1000 g on the samples (Fig. 4a).
(5) Samples were vacuum dried at 50 °C for 24 h.After curing, the force to take the PAM tablet off the Pb alloy sheet was measured as follows. The schematic diagram is shown in Fig. 4(b).
(6) A sample after drying was set on the adhesion measuring stage.

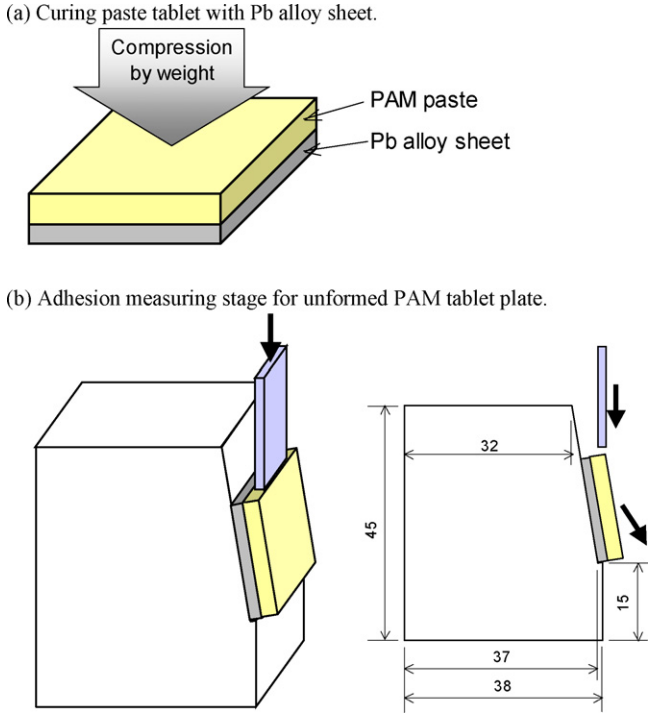

Fig. 4. Schematic diagram of curing the paste tablet with Pb alloy sheet and the adhesion measuring stage for the unformed PAM tablet plate sample after curing.

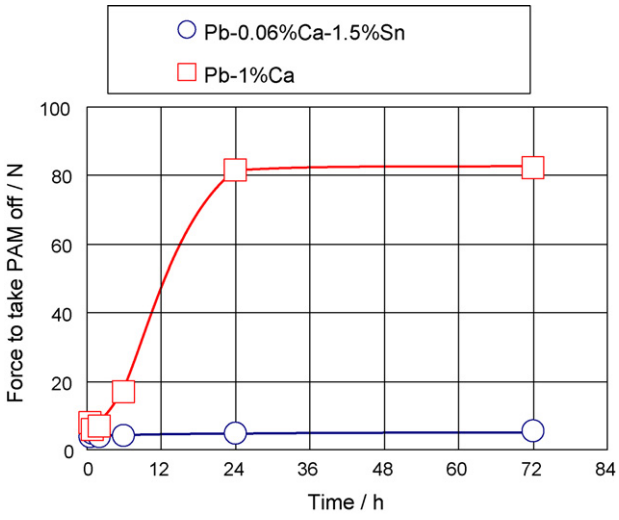

Fig. 5. Force to take the unformed PAM tablet off Pb sheet during curing with 24.5 kPa compression to the PAM/sheet interface. Composition of the sheet was Pb–0.06%Ca–1.5%Sn (◯) and Pb–1%Ca (□).

(7) Steel plate of 2 mm thick × 11 mm wide was lowered with 10 mm min^{-1} speed, as illustrated in Fig. 4(b).
(8) The force worked to the steel plate was measured by load cell set on it, at taking the PAM tablet off the Pb alloy sheet.

Each test was repeated for three samples and average force to take off was calculated.

3.2. Results and discussion

Fig. 5 shows the force to take the cured PAM tablet off the Pb alloy sheet after curing for various times. It shows that adhesion between the unformed PAM and Pb–1%Ca alloy begin to increase after 2 h from the start of curing. The force to take the PAM tablet off the sheet after 24 h exceeded 80 kPa, and was almost the same after 72 h. Therefore, adhesion of the PAM to the sheet become tight enough after 24 h curing. On the other hand, the force to take the PAM tablet off the Pb–0.06%Ca–1.5%Sn alloy sheet was less than 10 kPa even after 72 h curing. Adhesion to the Pb–0.06%Ca–1.5%Sn alloy sheet did not become tight under these conditions.

Fig. 6 shows the relationship between the compression to the PAM tablet/various alloy sheet interface during curing and the adhesion. The force to take the PAM tablet off increased when the compression increased. For Pb–0.06%Ca–1.5%Sn alloy, force data “0” means that the PAM came off before setting the sample on the measuring stage. Adhesion between the PAM and the Pb–1%Ca or Pb–5%Sb alloy is much higher than Pb–0.06%Ca–1.5%Sn alloy, especially cured with compression. Fig. 7 shows the photograph of the sheet samples after taking the PAM off. Pb–0.06%Ca–1.5%Sn sample was metallic lead color and relatively smooth. It means that the sheet surface was little corroded. Contrary, the surface of the Pb–1%Ca or Pb–5%Sb sheets was clearly covered by the oxide layer. The oxide corrosion layer is presumed to play role as glue in the interface.

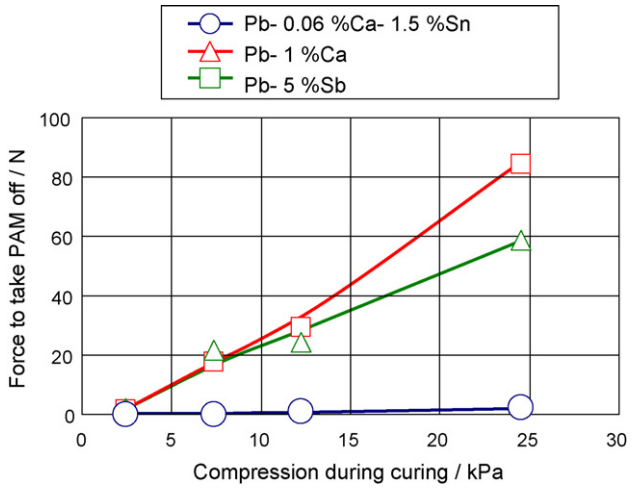

Fig. 6. Force to take the unformed PAM tablet off Pb alloy sheet after curing with various compression to the PAM/sheet interface. Composition of the sheet was Pb–0.06%Ca–1.5%Sn (◯), Pb–1%Ca (□), and Pb–5%Sb (△).

Corrosion layer of Pb alloy sheet after taking the PAM tablet off was analyzed by X-ray diffraction analysis (XRD). Fig. 8 shows the XRD pattern of corrosion layer on Pb–0.06%Ca–1.5%Sn (Fig. 8a), Pb–1%Ca (Fig. 8b), and Pb–5%Sb (Fig. 8c) after 24 h curing. Each corrosion layer after curing was found to consist of PbO, PbO hydrate, $PbSO_4$, and 3BS. The peak intensity for metal lead (m-Pb) on Pb–0.06%Ca–1.5%Sn was higher than on Pb–1%Ca or on Pb–5%Sb compared with peaks for PbO. It shows that the corrosion layer on Pb–0.06%Ca–1.5%Sn is thinner because Pb–0.06%Ca–1.5%Sn alloy can resist corrosion, however, it also means that the alloy is less adhesive to the PAM oxide tablet through the corrosion layer. On the other hand, the peak intensity for metal lead (m-Pb) on Pb–1%Ca was lower than on Pb–5%Sb. It shows that Pb–1%Ca is more corrosive and is more adhesive to the PAM through the corrosion layer than Pb–5%Sb. They are consistent with the adhesion measurement results.

It was found out that Pb–1%Ca as well as Pb–Sb alloy could make the adhesion tight between the PAM and the grid in the positive plates.

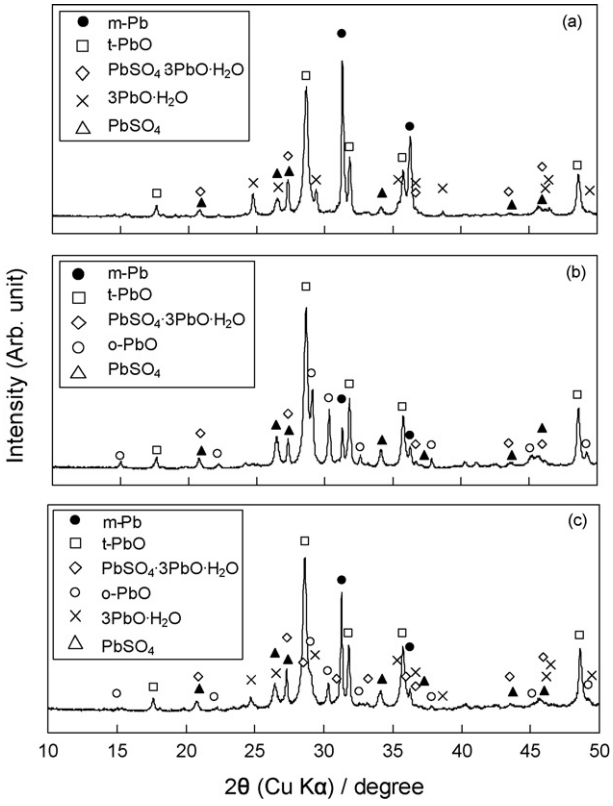

Fig. 8. X-ray diffraction pattern of current collector surface of; (a) Pb–0.06%Ca–1.5%Sn; (b) Pb–1%Ca; (c) Pb–5%Sb; after taking the PAM off after curing for 24 h at 50 °C, 80% relative humidity, with compression of 24.5 kPa.

4. Changes of interfacial states between the PAM and grid during cycling

The changes in the composition of the corrosion layer at the interface between the current collector and the PAM during the test cycle were examined.

4.1. Experimental

Electrodes with PAM (diameter: φ20 mm, thickness: 3 mm, density: 3.7 g cm^{-3}) on a Pb alloy current collector were man-

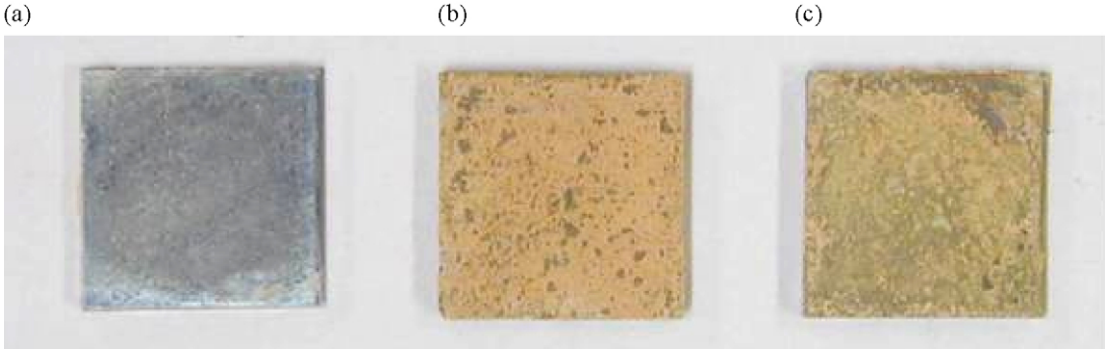

Fig. 7. Photograph of Pb alloy sheets surface after taking the PAM tablet off. Curing conditions were 24 h at 50 °C, 80% relative humidity, with compression of 24.5 kPa. Composition of the sheet was (a) Pb–0.06%Ca–1.5%Sn, (b) Pb–1%Ca, and (c) Pb–5%Sb.

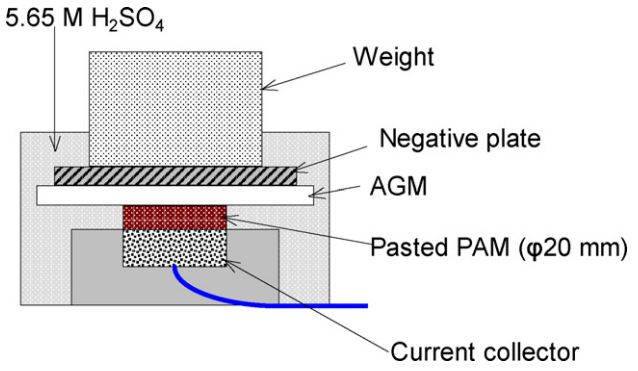

Fig. 9. Schematic diagram of the experimental cell for cycle test with PAM pasted directly on a current collector.

ufactured, as shown in Fig. 9. The PAM paste made from leady oxide powder, water and sulfuric acid was pasted on a Pb alloy current collector directly. Next, it was cured for 24 h at 50 °C, 80% relative humidity with compression of 24.5 kPa, and formed with compression by electrochemical oxidation to a PAM tablet on the current collector. Then, an AGM separator, a negative plate of larger capacity than that of the positive electrode with PAM and a 1000-g weight were put on it, and 5.65 M H_2SO_4 was poured into the cell. In this way, 300 mAh capacity cells were constructed. The cells were subjected to the cycling test of discharge with 100 mA for 20 min and charge with 15 mA for 200 min at 50 °C. The samples were picked out at planned cycles and chemical composition of the corrosion layer at the current collector/PAM interface was measured. Cells with current collectors of Pb–3%Sb–0.25%As alloy and Pb–1%Ca alloy were also tested.

The chemical composition of the corrosion layer was analyzed by the XRD. The characteristic diffraction line for α-PbO_2 was $2\theta = 28.58°$ and those for β-PbO_2 are $2\theta = 25.42°$ and $2\theta = 31.94°$. Intensity ratio of α-PbO_2 peak to sum of those of α-PbO_2 and β-PbO_2 was calculated as $Ip_{28.58°}/[Ip_{28.58°} + (Ip_{25.42°} + Ip_{31.94°})/2]$. The PAM was taken off the sample electrode, the current collector with corrosion layer on the surface was washed by distilled water, and the XRD of the surface was measured.

4.2. Results and discussion

The changes of the cell voltage at the end of discharge during cycling are shown in Fig. 10. The discharge voltage quickly decreased after only 35 cycles for the cell of Pb–0.06%Ca–1.5%Sn alloy current collector, although it did not decrease for the cells of both the Pb–3%Sb–0.25%As and the Pb–1%Ca alloy current collector. PCL was prevented on these types of alloy.

Examples of the XRD charts of the current collector surface after taking the PAM off are shown in Fig. 11. It shows the composition of the corrosion layer after the formation before the cycle test. The peak intensity for metal lead (m-Pb) on Pb–0.06%Ca–1.5%Sn was higher than on Pb–1%Ca or on Pb–3%Sb–0.25%As compared with peaks for PbO_2. This tendency was also observed in Fig. 8, on the electrode surface after curing before formation. It means that Pb–0.06%Ca–1.5%Sn alloy corrodes less than Pb–1%Ca or on Pb–Sb not only in cured positive electrodes but also in formed ones in cells. The changes in α-PbO_2 peak intensity

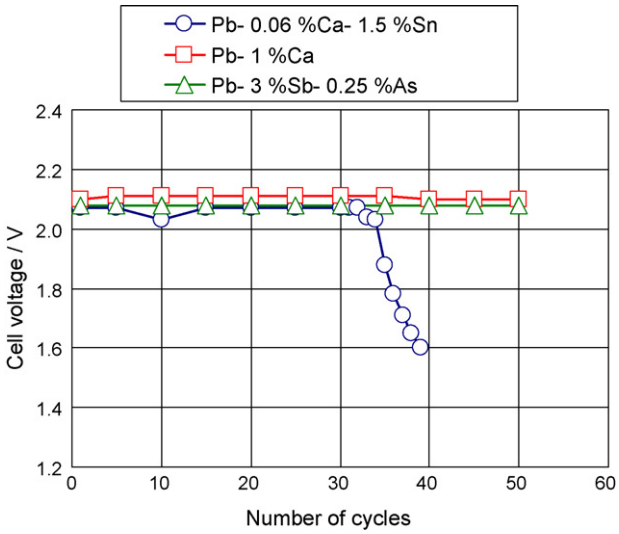

Fig. 10. Change in the end-of-discharge voltage of 300 mAh cells during PCL pattern cycle of the pasted tablet PAM cells. Composition of current collector alloy was Pb–0.06%Ca–1.5%Sn (◯), Pb–1%Ca (□), and Pb–3%Sb–0.25%As (△).

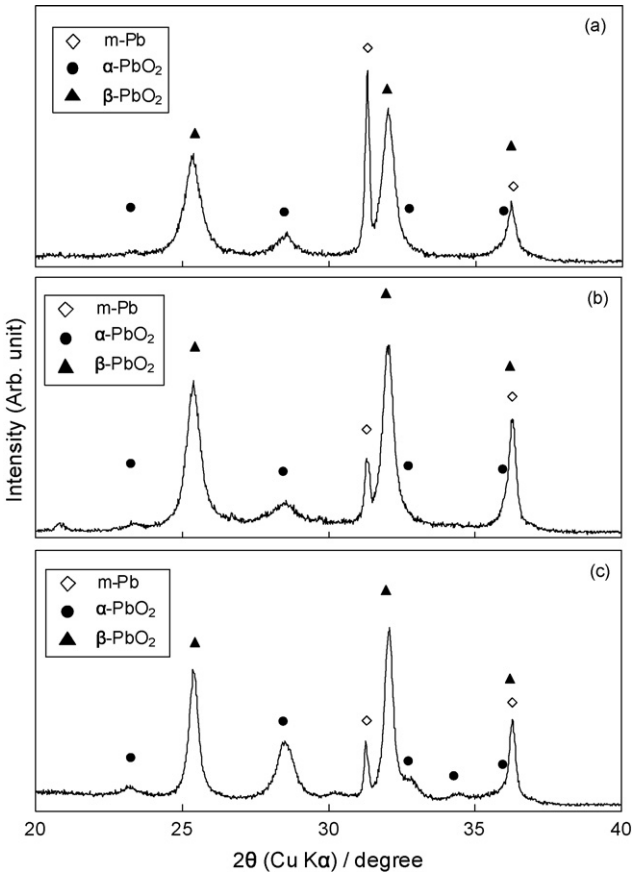

Fig. 11. X-ray diffraction pattern of surface of current collector surface of; (a) Pb–0.06%Ca–1.5%Sn; (b) Pb–1%Ca; (c) Pb–3%Sb–0.25%As; after taking the PAM off after PCL pattern cycle test.

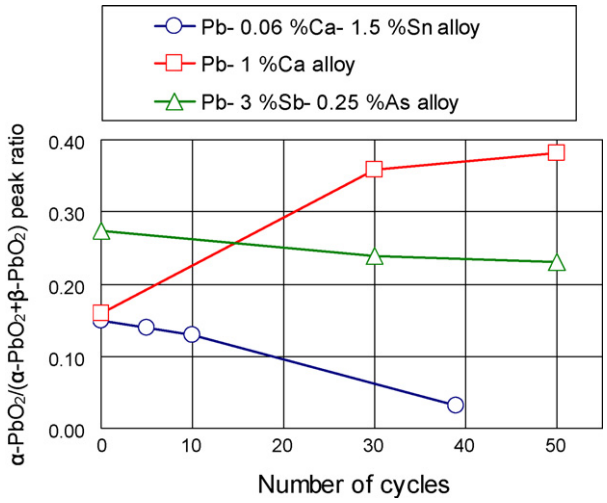

Fig. 12. Change in peak intensity ratio of α-PbO_2 to (α-PbO_2 + β-PbO_2) of the XRD, calculated as $Ip_{28.58°}/[Ip_{28.58°} + (Ip_{25.42°} + Ip_{31.94°})/2]$ of current collector surface after taking the PAM off. Composition of current collector alloy was Pb–0.06%Ca–1.5%Sn (◯), Pb–1%Ca (□), and Pb–3%Sb–0.25%As (△).

ratio to (α-PbO_2 + β-PbO_2) peak intensity of the XRD, calculated as $Ip_{28.58°}/[Ip_{28.58°} + (Ip_{25.42°} + Ip_{31.94°})/2]$ are shown in Fig. 12. Before cycling, the α-PbO_2 peak intensity ratio for Pb–0.06%Ca–1.5%Sn was almost the same as that for Pb–1%Ca and was less than that for Pb–3%Sb–0.25%As. It means that α-PbO_2 is relatively stable on Pb–Sb alloy before cycling, and that β-PbO_2 tends to be formed on Pb–Ca (–Sn) alloy under these conditions.

The peak ratio of α-PbO_2 to β-PbO_2 significantly decreased only for the Pb–0.06%Ca–1.5%Sn alloy electrode during cycling. On the other hand, the α-PbO_2 peak intensities for Pb–3%Sb–0.25%As alloy electrode held constant, and that for Pb–1%Ca alloy was increased during cycling. More stable phase of PbO_2 tends to increase by oxidation and reduction reaction during cycling on the current collector. Therefore, β-PbO_2 is increased on Pb–0.06%Ca–1.5%Sn alloy and is not increased on Pb–3%Sb–0.25%As alloy. On Pb–1%Ca alloy, it is assumed that α-PbO_2 become stable because H_2SO_4 concentration on the surface becomes lower, perhaps caused by its thick oxide layer and tighter adhesion at the interface.

It is well known that a Pb–Sb alloy positive grid can suppress PCL phenomenon. This might causes that the amount of α-PbO_2 in the corrosion layer on a Pb alloy grid did not decrease with the number of cycles.

As a result of these tests, it was found that Pb–1%Ca alloy current collector could prevent PCL, because of its increasing composition of α-PbO_2 in the corrosion layer during the cycles. It might be caused by its thick oxide layer and tighter adhesion at the interface.

5. Battery tests

It has become clear that it is effective for PCL prevention to apply Pb–1%Ca alloy to the positive grid for tight adhesion between the PAM and grid. Therefore, it was demonstrated in battery tests. It is difficult to apply this type of alloy to the positive grid by casting. It is because that Pb–1%Ca alloy is highly corrosive in sulfuric acid, so the battery life will be controlled by grid corrosion before PCL phenomenon. Therefore, the alloy technology was applied to expanded grid by laminating Pb–1%Ca foil on the Pb–0.06%Ca–1.5%Sn alloy thick cast sheet and rolling it to thin sheet for expanding.

5.1. Experimental

5.1.1. Test cell

2 V 8 Ah (5 hR) valve regulated cells were assembled with four positive plates and five negative plates and AGM separator. Electrolyte was 5.65 M (specific gravity 1.32 at 20 °C) H_2SO_4.

The types of the positive plates are shown in Table 2. Each positive expanded grid was designed in the same size and mass. The positive active material of 3.7 g cm^{-3} density was filled by the same mass for each type of grid.

The positive grids for the cell No. 2 were prepared as follows. Pb–1%Ca foil was laminated on the Pb–0.06%Ca–1.5%Sn alloy thick cast sheet and rolled with the cast sheet to thin sheet. The rolled sheet was expanded to the grid form, shown in Fig. 13(a). Fig. 13(b) shows the photograph of the cross section of the grid. Pb–1%Ca foil was laminated on the grid surface in 20 μm thick.

The positive grids for the cell No. 3 were prepared by the same way as the cell No. 2, but Pb–1.2%Sb–0.25%As alloy was chosen for laminated foil. The Sb content was set at as low as 1.2%, because Sb would lower the cell performance if the Sb content was high in VRLA battery.

5.1.2. Test regime

First, initial discharge capacity of each cell was checked. The cells were discharged at 1/3 CA (2.7 A) at 25 °C. The end of discharge voltage was set at 1.7 V. Then, the cells were tested under constant current charge–discharge cycle conditions at 50 °C. Cycle regime was designed to enhance PCL phenomenon. It is as follows.

Discharge: 1.5 A × 1.5 h (28% DOD).
Charge: 1.5 A × 1.2 h + 0.25 A × 5 h (135%).
Rest: 6 h.

Table 2
The test cell structure for PCL pattern life test

Cell No.	Positive grid type	Positive grid alloy	Negative grid type	Negative grid alloy
1	Expanded	Pb–0.06%Ca–1.5%Sn	Cast	Pb–Ca–Sn
2	Expanded	Pb–1%Ca foil laminated on Pb–0.06%Ca–1.5%Sn	Cast	Pb–Ca–Sn
3	Expanded	Pb–1.2%Sb–0.25%As foil laminated on Pb–0.06%Ca–1.5%Sn	Cast	Pb–Ca–Sn

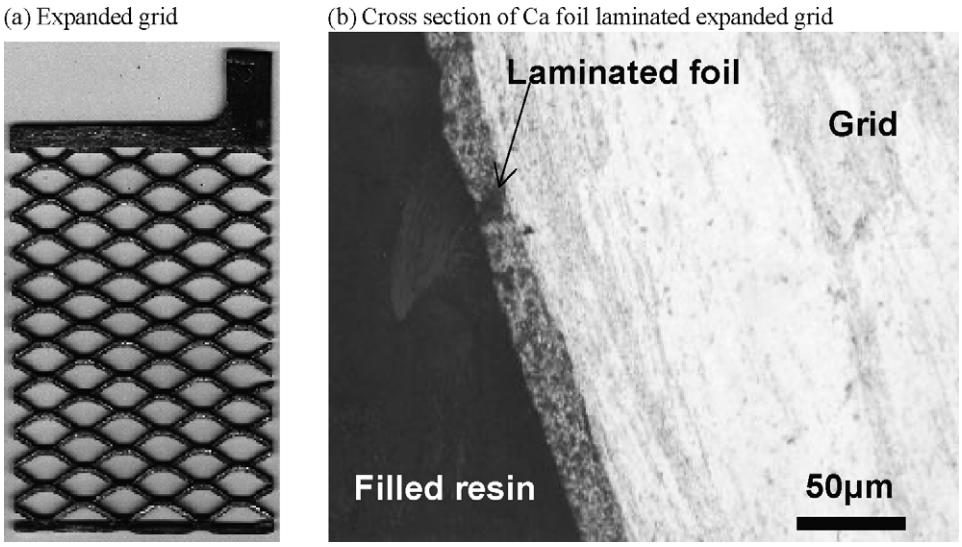

Fig. 13. Photographs of (a) expanded positive grid for 2 V 8 Ah test cell and (b) cross section of the positive grid surface laminated with Pb–1%Ca foil.

2.7 A discharge capacity was checked at 25 °C, at the 29th, 65th and 105th cycle of the charge–discharge cycle. The cells were charged at 0.8 A to 135% of discharged capacity.

5.2. Results and discussion

Fig. 14 shows the cell capacity change with PCL charge–discharge cycles. The initial capacity of each cell was almost the same. The cell No. 1, Pb–0.06%Ca–1.5%Sn positive grid without laminated foil, lost the capacity at the 29th cycle by PCL. The cell No. 3 with Pb–1.2%Sb–0.25%As laminated foil had longer life than the cell No. 1, but was deteriorated by PCL at the 105th cycle. On the other hand, the cell No. 2 with Pb–1%Ca laminated foil lived longer life than 105 cycles and showed an excellent durability against PCL.

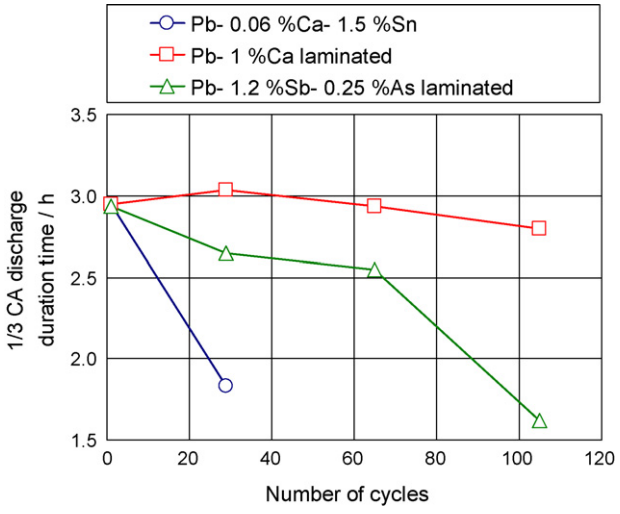

Fig. 14. Change in the capacity of 2 V 8 Ah cells during PCL pattern cycle. Discharge current was 2.7 A (3 CA), end of discharge voltage was 1.7 V. The positive grid was Pb–0.06%Ca–1.5%Sn without laminate (◯), Pb–1%Ca foil laminated (□), and Pb–1.2%Sb–0.25%As foil laminated (△).

It was found that the positive grids with Pb–Ca alloy laminated foil can prevent cycle use batteries from PCL and give them longer life.

6. Conclusions

(1) PCL occurs when the adhesion between the grid and the PAM is poor, the H_2SO_4 concentration at the interface between the grid or the PAM is high and the corrosion layer mainly consists of β-PbO_2.
(2) Pb–1%Ca alloy as well as Pb–Sb alloy can make the adhesion tight between the PAM and grid in the positive plates after curing.
(3) Pb–1%Ca alloy current collector could prevent PCL, because of its increasing composition of α-PbO_2 in the corrosion layer during the cycles. It might be caused by its thick oxide layer and tighter adhesion at the interface.
(4) The beneficial effect of Pb–1%Ca alloy grid on PCL was confirmed also in the battery cycle test. Ca ion does not lower the hydrogen overpotential at the negative electrode, resulting in less water loss in battery than Sb ion. Therefore, it can be applied to cycle use batteries.

References

[1] G. Karlsson, Proceedings of the 21st International Telecommunication Energy Conference, Copenhagen, Denmark, 6–9 June, 1999, pp. 21–23.
[2] M. Shiomi, Y. Okada, Y. Tsuboi, S. Osumi, M. Tsubota, J. Power Sources 113 (2003) 271.
[3] A.F. Hollenkamp, J. Power Sources 36 (1991) 567.
[4] M.K. Dimitrov, D. Pavlov, J. Power Sources 46 (1993) 203.
[5] Y. Okada, K. Takahashi, M. Tsubota, Proceedings of the 11th International Electric Vehicle Symposium, Florence, Italy, 27–30 September, 1992, p. 6.01.
[6] S. Laihonen, T. Laitinen, G. Sundholm, A. Yli-Pentti, Electrochim. Acta 35 (1990) 229.
[7] D. Berndt, Maintenance-Free Batteries, second ed., Wiley, 1997.
[8] D. Pavlov, G. Petkova, M. Dimitrov, M. Shiomi, M. Tsubota, J. Power Sources 87 (2000) 39.

[9] M. Dimitrov, D. Pavlov, J. Power Sources 93 (2001) 234.
[10] M. Kosai, S. Yasukawa, S. Osumi, M. Tsubota, J. Power Sources 67 (1997) 43.
[11] M. Tsubota, S. Osumi, M. Kosai, J. Power Sources 33 (1991) 105.
[12] A. Winsel, E. Voss, U. Hullmeine, J. Power Sources 30 (1990) 209.
[13] W. Borger, U. Hullmeine, H. Laig-Horstebrock, E. Meissner, in: T. Keily, B.W. Baxter (Eds.), International Power Sources Symposium Committee, Power Sources, vol. 12, Leatherhead, UK, 1989, p. 131.
[14] E. Meissner, J. Power Sources 46 (1993) 231.
[15] M. Calabek, K. Micka, P. Baca, P. Krivak, V. Smarda, J. Power Sources 64 (1997) 123.
[16] B.K. Mahato, J. Electrochem. Soc. 126 (1979) 365.
[17] B. Monahov, D. Pavlov, J. Electrochem. Soc. 141 (1994) 2316.
[18] M. Shiota, Y. Yamaguchi, Y. Nakayama, N. Hirai, S. Hara, J. Power Sources 113 (2003) 277.
[19] D. Pavlov, J. Power Sources 46 (1993) 171.
[20] M. Metikos-Hukovic, R. Babic, S. Brinic, J. Power Sources 64 (1997) 13.
[21] D. Pavlov, J. Electrochem. Soc. 139 (1992) 3075.
[22] T. Rogachev, J. Power Sources 23 (1988) 331.
[23] P. Ruetschi, B.D. Cahan, J. Electrochem. Soc. 104 (1957) 406.
[24] S. Ikari, S. Yoshizawa, S. Okada, Denki Kagaku 27 (1959) 552.